Electrical Engineering in Japan, Vol. 135, No. 3, 2001
Translated from Denki Gakkai Ronbunshi, Vol. 120-D, No. 4, April 2000, pp. 526–531

Characteristics of Short Primary Linear Induction Motor with a Partially Adopted Wound Secondary Member

YUSHI KAMIYA, KOJI FUKAYA, JEON WOOJIN, and TAKASHI ONUKI
Waseda University, Japan

SUMMARY

This paper describes single-sided linear induction motors (LIMs) with a short primary member. In these machines a solid-plate conductor is usually used for the secondary. We here propose the partial adoption of wound secondary members in LIMs. The characteristics of such machines are summarized as follows.

1. Basic characteristics: The wound secondary shortens the magnetic clearance and makes the characteristics of the machine superior to those of the solid-plate conductor version. In addition, we can improve the thrust and efficiency characteristics by applying the proportional shifting method.

2. Primary and secondary winding scheme: Parallel connection is appropriate for the primary and independently shorted-circuit scheme in order to obtain stable performance.

3. Transient phenomena at the boundary between the wound secondary and the solid-plate secondary: Undesirable phenomena develop at the boundary, especially at the end of the solid-plate conductor. Thus, we propose a novel boundary structure that yields stable transient performance.

Key words: Linear induction motor; wound secondary; FEM; electric circuit analysis; end effect.

1. Introduction

At present, most linear motors employed in transportation systems and in various vehicles are short primary linear induction motors (LIMs) [1]. With such motors, a secondary member must be laid across the whole operating area; usually, it is a massive conducting plate made of aluminum or some other metal. However, so long as a massive conductor is used, the magnetic gap inevitably grows long, hindering the improvement of performance. This study suggests the introduction of a wound secondary [2] into LIMs to improve their characteristics. With this design, the secondary resistance may be varied arbitrarily by inserting an external resistor; therefore, the characteristics may be controlled. In particular, an appropriate thrust or braking force may be achieved at the desired speed by using the proportional transition effect of induction machines. To realize such possibilities, this study suggests the application of a wound secondary to sections that involve starting/braking operations or that require strong thrust [3].

In this paper, the following subjects are examined using a combined analysis that includes FEM analysis of the electromagnetic field and driving circuit analysis, as well as tests with an experimental machine.

1. Basic characteristics of wound secondary LIMs.
2. Influence of the primary/secondary winding connection pattern on performance.
3. A new design proposed in order to explore transient phenomena that occur at the boundary of the massive conductor, and to improve performance.

2. LIM with Partially Adopted Wound Secondary

The configuration of a LIM with a wound secondary member as considered in this study is shown in Fig. 1. This is a short primary single-sided machine, with the secondary composed of massive conductor sections and wound sections. In the wound secondary design, the secondary contains windings inserted in core slots, as with the primary, while the secondary resistance may be varied by connecting an external resistor. Figure 2 shows an experimental machine, and its parameters are given in Table 1. The primary includes four poles, with the phases delta-connected.

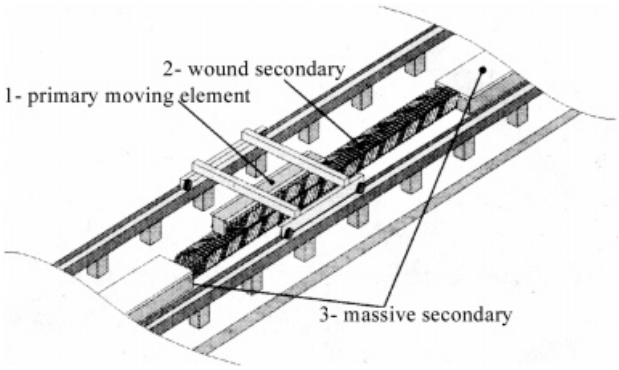

Fig. 1. Configuration of LIM with wound secondary.

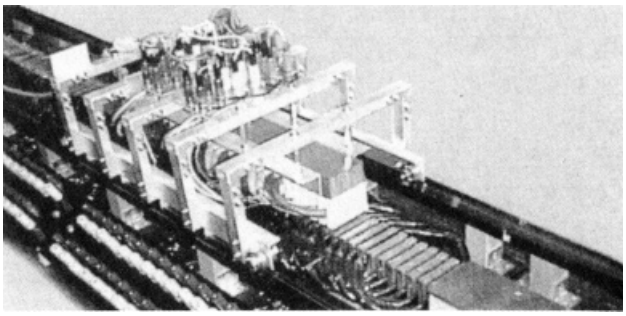

Fig. 2. Experimental machine.

Table 1. Parameters of experimental machine

Parameter	Designation	Value	Units
Core width	W_e	0.050	[m]
Pole pitch	τ	0.084	[m]
No. of primary poles	P	4	
No. of primary coils	q	2	
No. of primary coil fractions	β	1	
Secondary conductor (copper) thickness	T_s	0.004	[m]
Secondary conductor width	W_s	0.090	[m]
Mechanical gap length	g	0.002	[m]
Rated frequency	f	20	[Hz]

3. Analytical Methods with Allowance for Operating Conditions of Experimental Machine

This study employs FEM-based electromagnetic field analysis combined with electric circuit analysis, which allows us to consider both constant voltage source conditions and the secondary winding circuit [4, 5]. Therefore, the primary and secondary currents I_p, I_s are treated as unknown quantities in addition to the observable physical quantity of the magnetic field, namely, the magnetic vector potential $\boldsymbol{A}$. The algorithm of this three-dimensional combined field/circuit analysis is described below.

3.1 Governing equation of magnetic field

Using the magnetic vector potential as the observable physical quantity in three-dimensional orthogonal coordinates, the governing equation is as follows:

$$\frac{\partial}{\partial x}\left(\frac{1}{\mu}\frac{\partial \boldsymbol{A}}{\partial x}\right)+\frac{\partial}{\partial y}\left(\frac{1}{\mu}\frac{\partial \boldsymbol{A}}{\partial y}\right)+\frac{\partial}{\partial z}\left(\frac{1}{\mu}\frac{\partial \boldsymbol{A}}{\partial z}\right)$$

$$=-\left(\boldsymbol{J}_p+\boldsymbol{J}_s\right)+\sigma\left(\nabla\phi+\frac{\partial \boldsymbol{A}}{\partial t}\right) \tag{1}$$

Here μ is the magnetic permeability, J_p is the primary current density, J_s is the secondary current density, σ is the conductivity, and ϕ is the electric scalar potential.

3.2 Circuit equation

For the purpose of constant-voltage driving circuit analysis, a circuit equation is introduced in addition to the governing equation of the electromagnetic field. With ν, Φ, and R denoting, respectively, the applied voltage, total linked flux, and coil resistance between terminals of delta-connected primary coils,

$$\frac{\mathrm{d}\Phi}{\mathrm{d}t}+R_p i_p=v \tag{2}$$

In the case of the secondary coils, the source is not considered. Hence,

$$\frac{\mathrm{d}\Phi}{\mathrm{d}t}+R_s i_s=0 \tag{3}$$

3.3 Coupling

The above equations are coupled in the following way. With the coil conductor cross-sectional area denoted by S_c, the coil effective area by S_e, the number of turns by N, and an element of length along the coil loop by dl, the following relations exist between current and current density, and between total linked flux and vector potential:

$$i = JS_c \tag{4}$$

$$\Phi = N\int_{S_e} \boldsymbol{B}\cdot \mathrm{d}\boldsymbol{S} = N\oint_l \boldsymbol{A}\cdot \mathrm{d}\boldsymbol{l} \tag{5}$$

The coexistence of Eqs. (1) to (5) makes possible the simultaneous calculation of the vector potential and the primary/secondary currents.

The analytical algorithm described above is employed in this study; in addition, the backward difference method is used for the time derivative term, and movement of the moving part is represented by time-stepping [6].

4. Characteristics of Wound LIM

4.1 Basic characteristics

In this section, analysis and experiments are used to compare the wound secondary LIM to the conventional (massive conductor) LIM in terms of basic characteristics, and to demonstrate the advantages of the former design.

The magnetic flux distributions at standstill for the wound secondary and massive secondary are shown in Fig. 3. Figures 4 and 5 present the thrust and efficiency characteristics, respectively. With the proposed design, the secondary includes coils inserted in core slots, as with the primary, hence the magnetic gap can be made shorter than in the massive secondary. Therefore, the magnetic coupling between the primary and secondary grows stronger, and the magnetic flux density increases in the gap. This also improves such mechanical characteristics as thrust and efficiency. Employing a ladderlike secondary also offers improved characteristics, but in the wound secondary design, the secondary resistance can be varied arbitrarily by using an external resistor, and the proportional transition effect contributes to better thrust performance, as confirmed by Fig. 4. For certain reasons to be explained in the next section, in these experiments the primary has fractional-pitch distributed windings connected in parallel for each pole, while the secondary has full-pitch windings short-circuited independently for each coil; a voltage of 4.8 V is supplied for each pole.

4.2 Primary/secondary winding connection

When the wound secondary is partially adopted in the short primary LIM, various phenomena may take place at the boundary of the plate conductor depending on the winding connection pattern, and inappropriate connection choice may impair performance. Hence, we consider below some primary/secondary winding connection patterns that ensure smooth movement across plate conductor sections and wound sections, as well as through their boundaries.

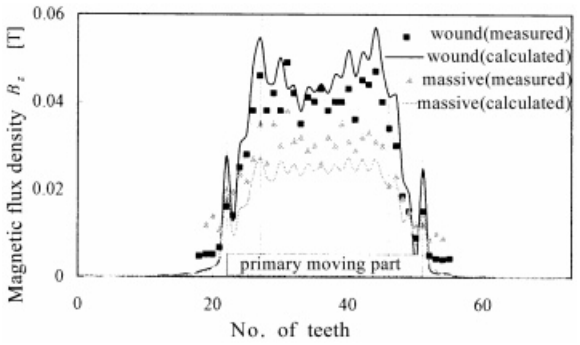

Fig. 3. Distribution of magnetic flux density in gap (at standstill).

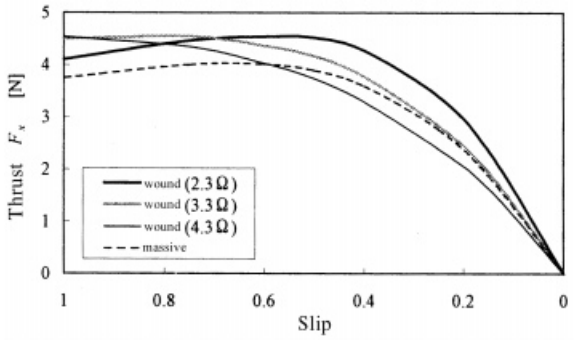

Fig. 4. Slip versus thrust characteristics.

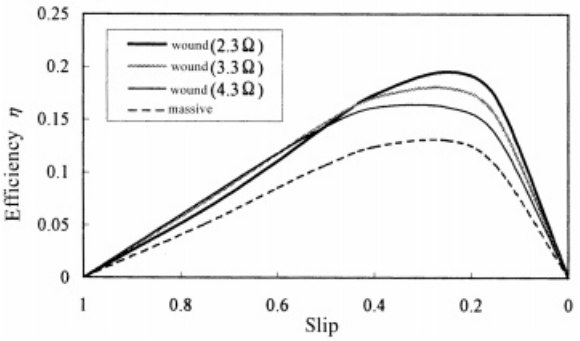

Fig. 5. Slip versus efficiency characteristics.

(1) Secondary winding connection

The LIM performance characteristics were compared for various connection patterns of secondary full-pitch coils. In these comparisons all poles in the primary windings were connected in parallel for each phase.

The following three connection patterns were considered.

(a) each coil is short-circuited independently;

(b) two coils located one pole apart are connected in series;

(c) three coils located one pole apart are connected in series.

In the case of independent short-circuit coils, the secondary current flows only through the coils that face the primary iron core. However, in a two- or three-pole series connection, the secondary current also flows through the coils that do not face the primary. Therefore, magnetic flux appears beyond the primary, compensating for the finite size of the primary in the short primary LIM, so that the thrust increases and stable traveling characteristics can be expected.

Figure 6 shows the secondary current distributions at standstill for different connection patterns, and Fig. 7 shows the magnetic flux density distribution.

In the independent short-circuited connection, the secondary current flows only through the secondary coil that faces the primary. However, since the connection involves two or three poles, a secondary current also flows through the coils located before and after the primary moving element, so that the current distribution takes the shape of a bell symmetrical about the moving primary center. In addition, with two- and three-pole connection, the secondary current distribution experiences greater pulsations than in short-circuited coils. This phenomenon is explained by the fact that the magnetic linkage flux depends heavily on the configuration of the series-connected coil groups. As regards the magnetic flux density, in two- and three-pole connection the distribution becomes valley-

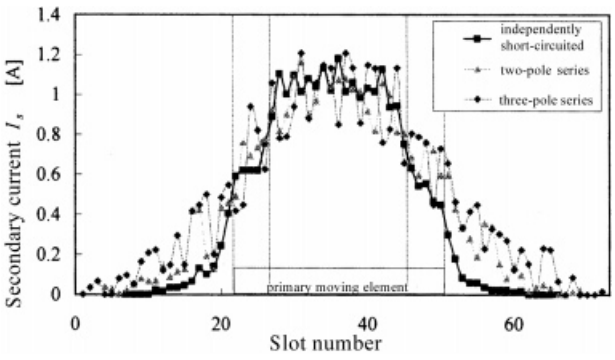

Fig. 6. Secondary current distribution (measured).

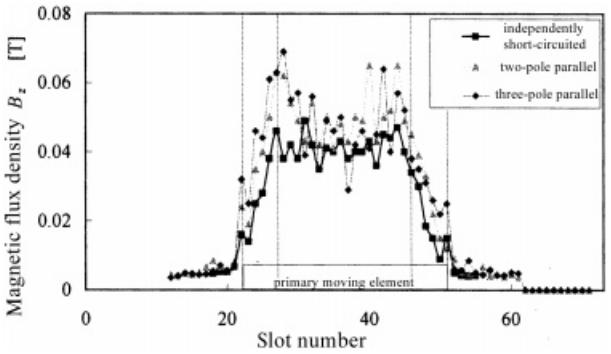

Fig. 7. Distribution of magnetic flux density in gap (measured).

shaped rather than bell-shaped, and the pulsations become larger as well.

The traveling performance was also examined in terms of thrust time variation, and it was found that series connection did not contribute to an increase in thrust or to suppression of pulsation; furthermore, the leakage flux impaired thrust (for details, see Ref. 3).

From the above results, we may conclude that independent short-circuited connection of secondary windings in a wound secondary LIM is appropriate in terms of stable performance and simple design.

(2) Primary winding connection

Comparative characteristics were obtained when primary coils of the same phase were connected in series, and when parallel connection was performed for all poles. In the case of the partially adopted wound secondary as proposed in this study, four cases are to be considered: (a) wound section with coils of the same resistance, (b) wound section with coils of different resistance, (c) boundary between wound section and massive conductor, and (d) massive conductor section. All of these cases were examined to find a primary winding connection pattern that guaranteed stable performance, but only case (b) is reported in this paper (for more details, see Ref. 3). The primary coils are assumed to be fractional-pitch windings, and the secondary windings are assumed to be short-circuited independently (proceeding from the results explained above).

The magnetic flux density distribution at standstill is shown in Fig. 8. In the case of parallel-connected primary windings, the difference in magnetic flux density distribution across the sections with different resistances is mitigated. The reason is that, as shown in Table 2, the primary current is nearly equal in all coils in the case of series connection; on the other hand, with parallel connection, the secondary current is much different for every phase and every pole, which provides a more uniform distribution of

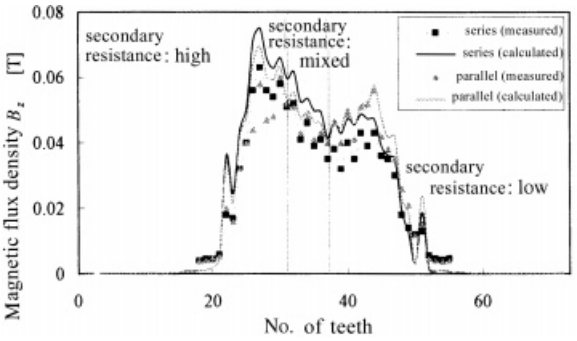

Fig. 8. Distribution of magnetic flux density (measured).

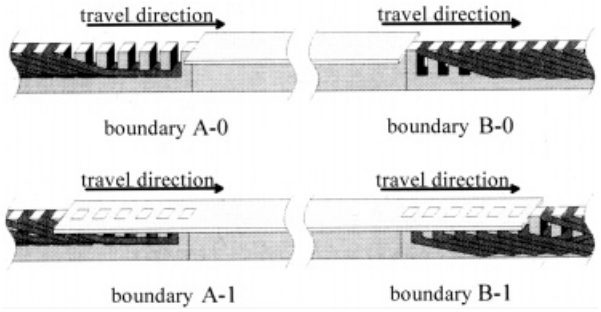

Fig. 9. Boundary structures.

the magnetic flux density. Thus, in the case of parallel connection, appropriate thrust and vertical force are applied to the primary moving element, and stable performance is obtained even when passing between different secondary sections. However, the capacitance of coil conductors must be designed carefully, since eddy currents may occur in the primary because of the edge effect and certain parameters of the secondary.

4.3 Transient characteristics at wound/massive boundary

When the wound secondary is partially adopted in a short primary LIM, complicated transient phenomena take place at the boundaries with the massive conductor sections, which may impair performance. In this study, such transient phenomena are examined in detail, and a new boundary design intended to achieve smooth transient characteristics is proposed.

The boundary structures under consideration are shown in Figs. 9 and 10. When the moving element passes a boundary, two cases are possible: from the wound section to the massive conductor section (boundary A), and the reverse, from the massive conductor section to the wound section (boundary B). In addition, two types of boundary structure may exist: with wound and massive sections just adjacent to each other (Type 0), and with ladderlike design (Type 1). The latter design is proposed in this study; in particular, conductors are inserted ladderwise in the empty slots of the single-layer portion of the wound section to produce smooth transitions. Four structures, A-0, A-1, B-0, and B-1, were examined. The primary coils were connected in parallel and the secondary coils were short-circuited

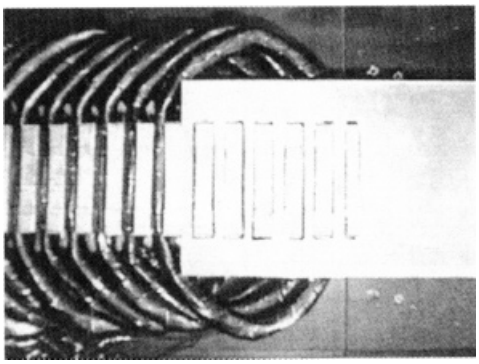

Fig. 10. Boundary A-1 structure.

Table 2. Primary current (analytical results)

	Constant resistance winding		Variable resistance winding		Wound/massive boundary	
	Series	Parallel	Series	Parallel	Series	Parallel
Average (A)	1.45	1.46	1.39	1.39	1.44	1.48
Minimum (A)	1.41	1.29	1.32	1.21	1.39	1.18
Maximum (A)	1.49	1.81	1.45	1.80	1.47	2.02

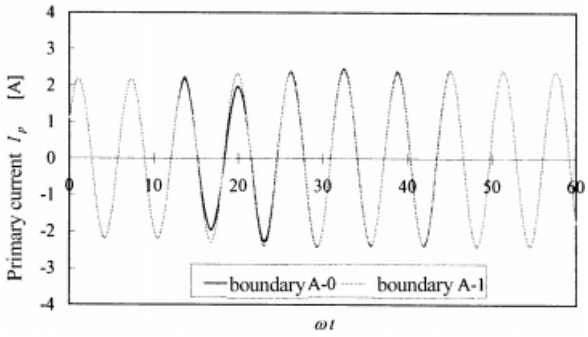

Fig. 11. Time variation of primary current.

independently (as was proven to be appropriate). The moving primary was assumed to cross the boundaries between sections at a slip of 0.5; therefore, the resistance of the secondary coils was designed so that the thrust at the wound sections and massive sections was nearly equal at this slip value.

The time variation of the current flowing through the primary coils when crossing boundary A is shown in Fig. 11, and Fig. 12 shows the time variation of the thrust. With a Type 0 boundary, the amplitude of the primary current decreases as the moving primary crosses the single-layer portion of the wound section. This is because the secondary current is lower here than in the double-layer portion. With Type 1, where the deficiency of the secondary current is compensated by eddy currents in the ladderlike conductor, the amplitude of the primary current does not decrease when a boundary is crossed, and a smooth transient characteristic can be achieved. On the other hand, the thrust fluctuates heavily when a Type 0 boundary is crossed, and its average decreases. This phenomenon may take a heavy toll on performance, and hence the authors tried to investigate it in more detail.

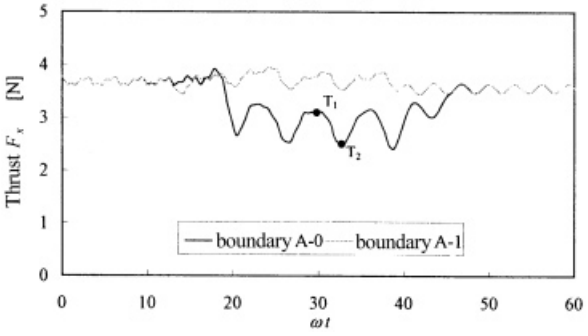

Fig. 12. Time variation of thrust.

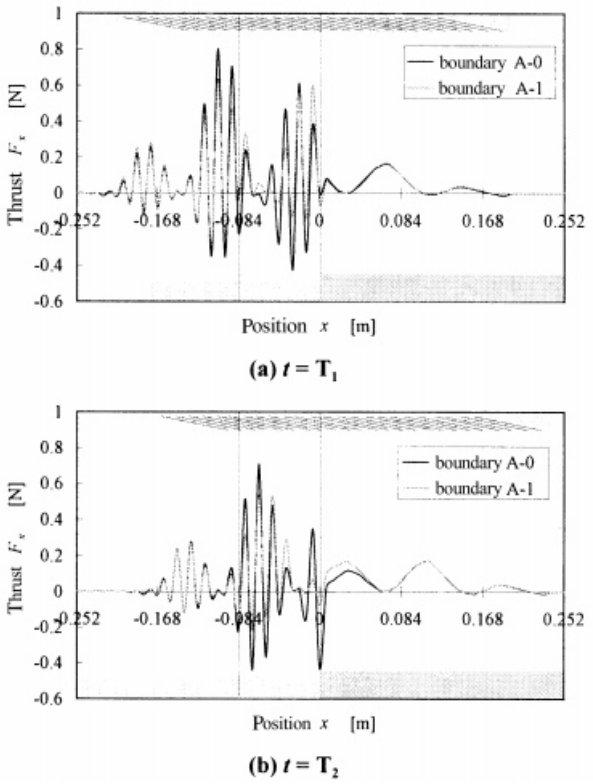

Fig. 13. Instantaneous thrust distribution.

Figures 13 and 14 show the distributions, respectively, of the thrust and secondary current at boundary A. In the diagrams, T_1 is the instant when the thrust reaches its maximum in a pulsation cycle, as shown in Fig. 12, and T_2 is the instant when the thrust reaches a minimum. In addition, in Fig. 14 longer arrows correspond to higher current densities. With Type 0 design, the eddy currents in the massive conductor are restricted, and hence smooth spiral flow is sometimes interrupted. As a result, backward thrust appears at the boundary, and the overall thrust drops. This transient phenomenon is observed at $t = T_2$. On the other hand, at $t = T_1$, the flow of eddy currents is smooth, and backward thrust does not appear at the boundary. Therefore, the thrust reaches its maximum. In addition, the secondary current is small in the single-layer portion of the wound section, so that only a small thrust is generated. Thus, basically, the thrust drops when the boundary is crossed. On the other hand, in the case of Type 1, the massive conductor portion overlaps the wound portion, so that generation of backward thrust is inhibited to some extent. At the same time, the deficiency of secondary current is compensated in the single-layer portion so that the thrust does not decline, and the performance remains stable. It follows from the above that when boundary A is crossed, the thrust drops

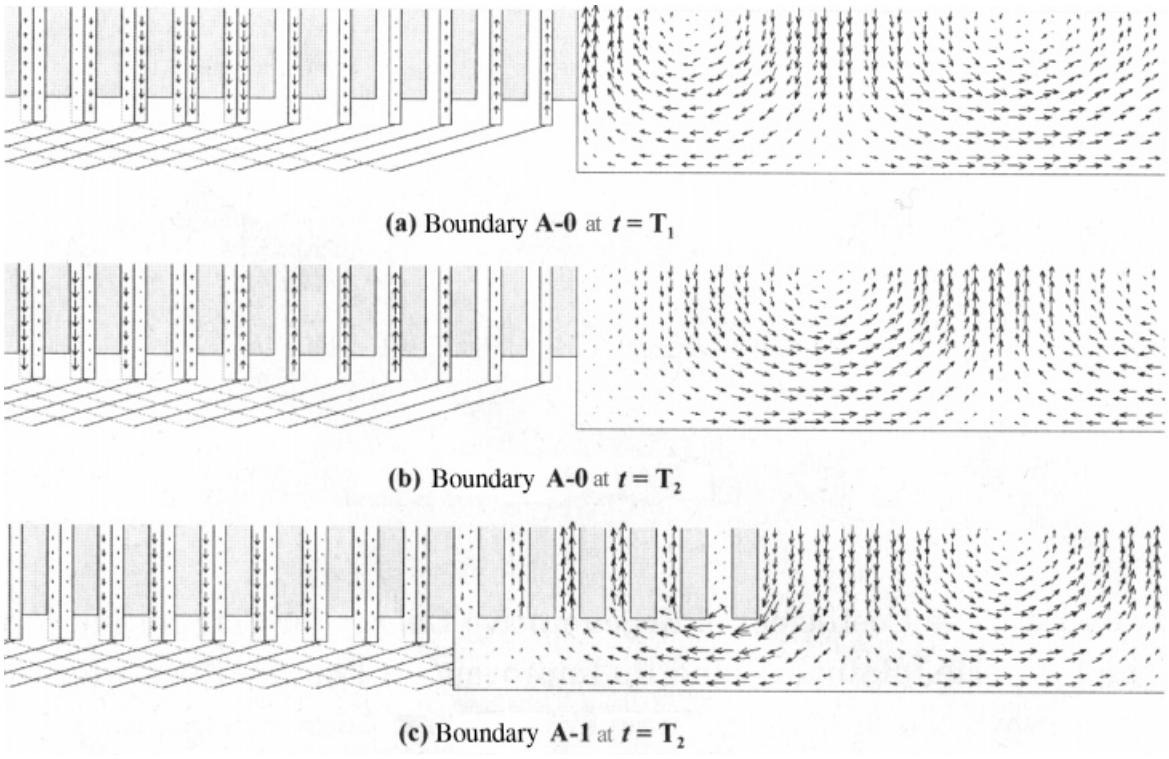

Fig. 14. Secondary current distribution.

because of the influence exerted by the single-layer portion of the wound section, and because of the backward thrust that appears periodically due to the edge effect at the massive conductor (at the outlet edge of the magnetic field); in addition, the pulsation increases. However, the phenomena that underlie this performance impairment are considerably reduced by adoption of Type 1, which proves the efficiency of the proposed design.

On the other hand, when boundary B is crossed, the thrust decreases of the influence exerted by the single-layer portion of the wound section, but the pulsation increases due to the edge effect at the massive conductor; in this case, too, the proposed design was proven to stabilize performance. However, results concerning boundary B are omitted here for reasons of space.

5. Conclusions

This study aims at improving the performance and controllability of single-sided short primary linear induction motors; for this purpose, partial adoption of wound secondary has been proposed, and the performance characteristics have been examined. In addition, the main points to be considered in the new design have been identified. The results obtained in the present study can be summarized as follows.

(1) Due to the adoption of a wound secondary, the magnetic coupling between the primary and secondary becomes stronger and such performance characteristics as thrust and efficiency are improved. In addition, the characteristics can be controlled by varying the secondary winding resistance.

(2) When a wound secondary is partially adopted, the best results are obtained with the secondary windings short-circuited independently and primary windings connected in parallel.

(3) When a moving part crosses a boundary between a wound section and a massive conductor section, the performance characteristics decline in the single-layer portion of the wound section and at the edge of the massive conductor. To improve the situation, a ladder-like boundary design has been proposed, and has proved to be effective.

The authors do not deny that the proposed design with wound secondary is relatively complicated. However, considering its excellent characteristics, this design may be worth using in specific sections where starting/braking operation is involved, or where a strong thrust is required (such as up-slopes).

Acknowledgment

The authors express their gratitude to Mr. T. Fujinami for his help in the experiments.

REFERENCES

1. Kusakari M, et al. Propulsion system for linear motor car. IEE Japan, Linear Drive Commission, LD-92-50, 1992.
2. Fujii N, et al. Study on efficient operation of linear motors for urban transportation. '92 Natl Conf IEE Japan, Industrial Section, Vol. 213-D, No. 12, p 877–882.
3. Onuki T, Kamiya Y, Iraha T, Fukaya K, Jeon W. Improvement of short primary member linear induction motor performance by partial adoption of the wound secondary. 33rd Annual Meeting of the Industry Applications Society, St. Louis, 1998.
4. Onuki T, et al. Study on primary coil connection in constant-voltage-driven short secondary linear induction motors. Trans IEE Japan 1996;116-D:1283–1288.
5. Kamiya Y, Onuki T. 3-D eddy current analysis by the finite element method using double node technique. IEEE Trans Magn 1996;32:741–744.
6. Preston TW, Reece ABJ, Sangha PS. Induction motor analysis by time-stepping techniques. IEEE Trans Magn 1988;24:471–474.

AUTHORS (from left to right)

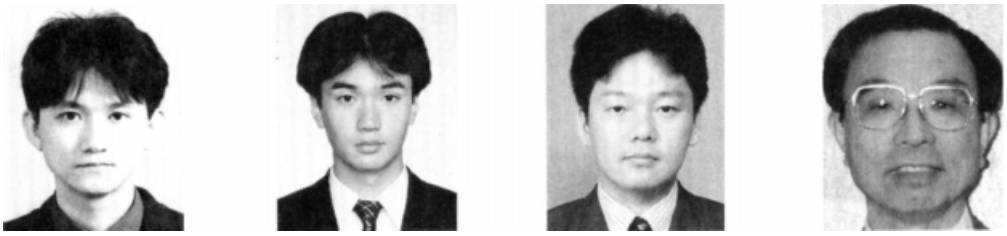

Yushi Kamiya (member) graduated from Waseda University (electrical engineering) in 1993 and completed his doctorate in 1997. He became a research associate at Waseda University in 1996 and a researcher at the Traffic Safety and Nuisance Research Institute (Ministry of Transport) in 1998. Since 2000 he has been an assistant professor at Gunma University. His research focuses on environment and energy. He was awarded a 1992 IEE Japan Paper Award.

Koji Fukaya (student member) graduated from Waseda University (electrical engineering) in 1998 and is now in the M.E. program. His research interests center on performance improvement of linear motors using numerical electromagnetic field analysis.

Jeon Woojin (member) graduated from Konkaku University (electrical engineering) in 1991 and completed the M.E. and doctoral programs at Waseda University in 1995 and 1998. He is now a research associate at Waseda University. He holds a D.Eng. degree. His research interests include special electric machines using numerical electromagnetic field analysis.

Takashi Onuki (member) graduated from Waseda University (electrical engineering) in 1951 and joined the Research Center of the Ministry of Commerce and Industry. He moved to the faculty of Waseda University in 1954 and has been a professor since 1968. He was director of the Physical Research Center from 1988 to 1992. He holds a D.Eng. degree. His research interests include linear motors and numerical analysis of electromagnetic fields. He received an IEEJ Paper Award in 1987. He is an IEEE Fellow.